

## DISCOVERY OF FOUR NEW MASSIVE AND DENSE COLD CORES

GUIDO GARAY, SANTIAGO FAÚNDEZ, DIEGO MARDONES, AND LEONARDO BRONFMAN  
Departamento de Astronomía, Universidad de Chile, Casilla 36-D, Santiago, Chile

ROLF CHINI

Astronomisches Institut der Ruhr-Universität Bochum, Universitätsstrasse 150, 44780 Bochum, Germany

AND

LARS-ÅKE NYMAN

European Southern Observatory, Alonso de Cordova 3107, Vitacura, Casilla 19001, Santiago, Chile

Received 2004 January 8; accepted 2004 March 25

### ABSTRACT

We report the identification, from a 1.2 mm dust continuum emission survey toward massive star-forming regions, of four strong 1.2 mm sources without counterparts at mid-infrared (*Midcourse Space Experiment* [*MSX*]) and far-infrared (*IRAS*) wavelengths. They have radii in the range 0.2–0.3 pc, dust temperatures  $\leq 17$  K, masses in the range  $4 \times 10^2$ – $2 \times 10^3 M_{\odot}$ , and densities of  $\sim 2 \times 10^5 \text{ cm}^{-3}$ . We suggest that these objects are massive and dense cold cores that will eventually collapse to form high-mass stars.

*Subject headings:* dust, extinction — ISM: clouds — ISM: molecules — stars: formation

### 1. INTRODUCTION

Surveys of molecular line emission in high-density tracers (Plume et al. 1992, 1997; Juvela 1996) and of dust continuum emission (Beuther et al. 2002; Mueller et al. 2002) made with single-dish telescopes have shown that massive stars form in regions of molecular gas with distinctive physical parameters, which we refer to as massive dense cores.<sup>1</sup> For example, from observations of the CS (5  $\rightarrow$  4) line emission toward massive star-forming regions associated with H<sub>2</sub>O masers, Plume et al. (1997) derived typical radii of 0.5 pc, densities of  $8 \times 10^5 \text{ cm}^{-3}$ , and virial masses of  $3.8 \times 10^3 M_{\odot}$  for massive dense cores. Whether or not these parameters are representative of the initial conditions for the formation of massive stars at the scale of parsecs is not clear. All of the above surveys have been carried out toward luminous sources, either ultracompact (UC) H II regions and/or luminous *IRAS* sources, implying that massive stars have already been formed within the core. For instance, the average luminosity of the sources in the samples of Plume et al. (1997) and Mueller et al. (2002) are  $9 \times 10^5$  and  $2 \times 10^5 L_{\odot}$ , respectively. Thus, the massive luminous embedded objects may have already appreciably affected their natal environment through stellar winds and radiation.

The observational evidence for massive dense cold cores, which are capable of forming massive stars but are in a stage before star formation actually begins, has been hard to find (see Evans et al. 2002). These cores should have similar densities and sizes to massive dense cores with embedded high-mass stars, but lower luminosities and cooler temperatures. The bulk of their luminosity is expected to be emitted at millimeter and submillimeter wavelengths. The recent availability of large bolometer arrays facilitating the observations of large-scale maps of dust continuum emission at millimeter wavelengths is allowing the search for promising candidates, namely millimeter sources without mid-IR and far-IR counterparts.

Faúndez et al. (2004) recently carried out a survey of 1.2 mm continuum emission toward a sample of 146 luminous objects with strong CS (2  $\rightarrow$  1) emission, chosen from the CS (2  $\rightarrow$  1) survey of Bronfman et al. (1996) of *IRAS* sources with IR colors typical of compact H II regions. The 1.2 mm emission was mapped within regions of  $\sim 15' \times 10'$  centered on the *IRAS* sources. A primary goal of this study was to determine the physical conditions of the dust and gas clouds harboring recently formed massive stars. In addition, since the sites of massive star formation are known to be gregarious, a further goal of this survey was to find massive cores in early stages of evolution, previous to the formation of a central massive object. In about half of the mapped regions, Faúndez et al. (2004) detected two or more distinct 1.2 mm sources, one of which is associated with the *IRAS* source. Using this database, we searched for candidates for massive dense cold cores by examining maps of the mid-IR emission from these regions taken from the *Midcourse Space Experiment* (*MSX*) and *IRAS* databases. In this paper we report the discovery of four 1.2 mm massive ( $M > 400 M_{\odot}$ ) dust cores not seen in emission at any of the *MSX* and *IRAS* wavelengths. We also report observations of molecular line emission toward three of these objects, which confirms that they are associated with massive and dense cold molecular cores.

### 2. OBSERVATIONS

The observations were made using the 15 m Swedish-ESO Submillimeter Telescope (SEST) at La Silla, Chile. The 1.2 mm continuum observations were made using the 37 channel SEST Imaging Bolometer Array (SIMBA) between 2001 June and 2002 July. The passband of the bolometers has an equivalent width of 90 GHz and is centered at 250 GHz. The half-power beamwidth (HPBW) of a single element is  $24''$ , and the separation between elements on the sky is  $44''$ . We observed in the fast mapping mode, using a scan speed of  $80'' \text{ s}^{-1}$ . Each observing block consisted of 50 scan lines in azimuth of length  $800''$  and separated in elevation by  $8''$ , giving a map size of  $400''$  in elevation. This block required  $\sim 15$  minutes of

<sup>1</sup> We here adopt the nomenclature of Evans (1999) for the use of the terms cores and clumps.

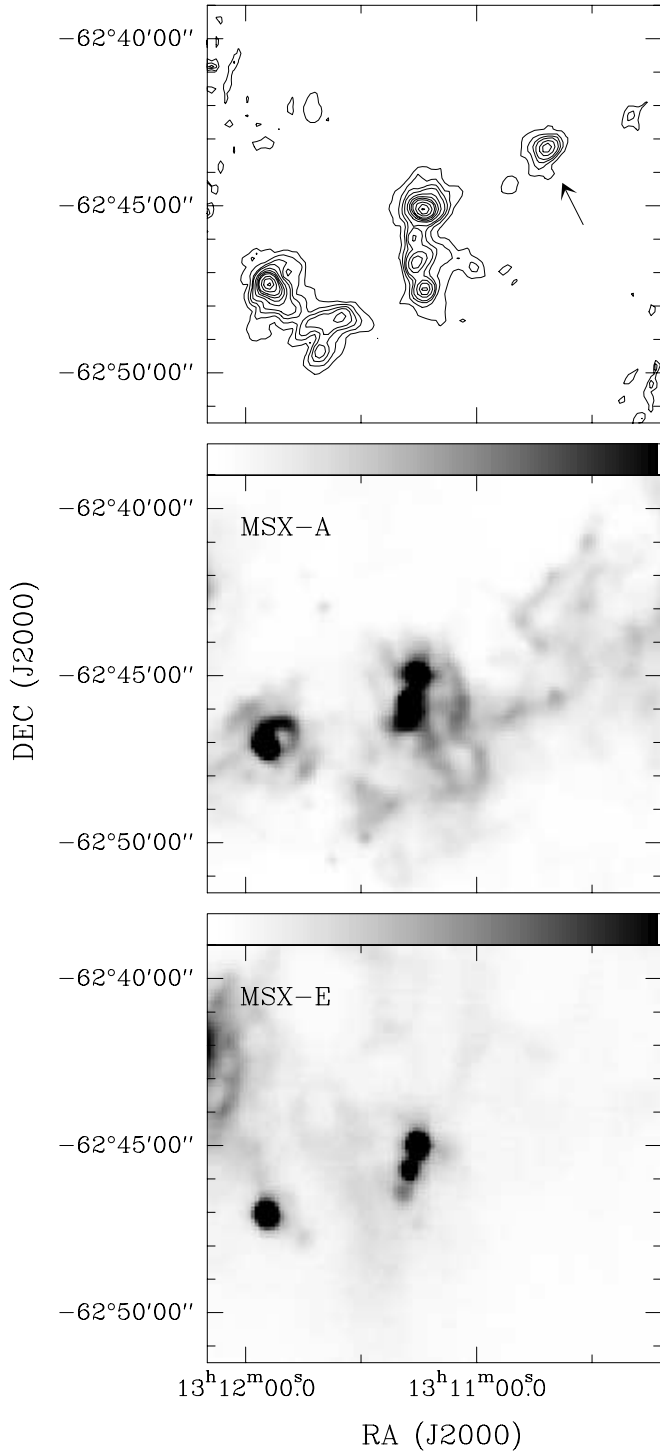


FIG. 1.—*Top*: Map of the 1.2 mm emission from a  $12' \times 12'$  region centered on IRAS 13080–6229. The arrow indicates the G305.136+0.068 massive and dense cold core. Contour levels are 1, 2, 3, 4, 6, 8, 10, 12, 16, 20, and  $24 \times 0.15 \text{ mJy beam}^{-1}$ . *Middle*: Image of the MSX emission in the A broad band ( $6.8\text{--}10.8 \mu\text{m}$ ). *Bottom*: Image of the MSX emission in the E broad band ( $18.2\text{--}25.1 \mu\text{m}$ ).

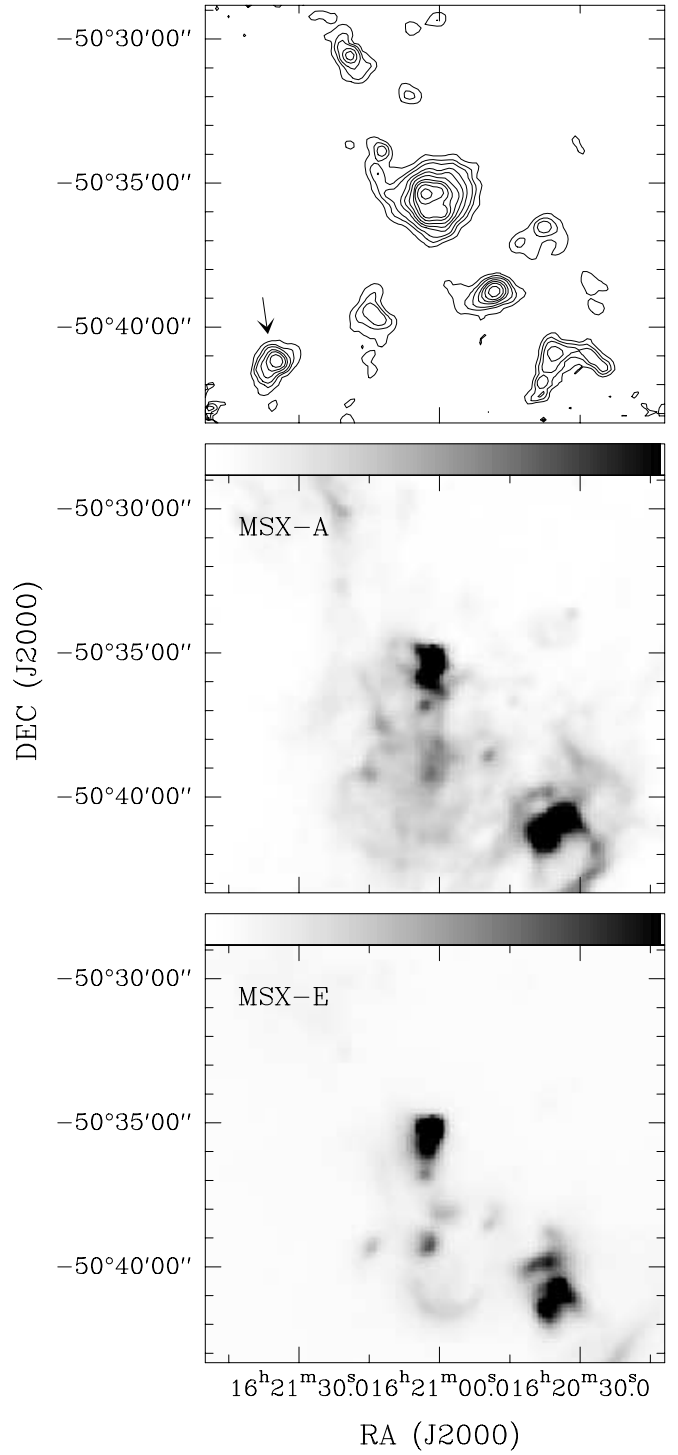


FIG. 2.—*Top*: Map of the 1.2 mm emission from a  $14' \times 14'$  region centered on IRAS 16172–5028. The arrow indicates the G333.125–0.562 massive and dense cold core. Contour levels are 1, 2, 3, 5, 7, 10, 15, 20, 30, and  $50 \times 0.18 \text{ mJy beam}^{-1}$ . *Middle*: Image of the MSX emission in the A broad band ( $6.8\text{--}10.8 \mu\text{m}$ ). *Bottom*: Image of the MSX emission in the E broad band ( $18.2\text{--}25.1 \mu\text{m}$ ).

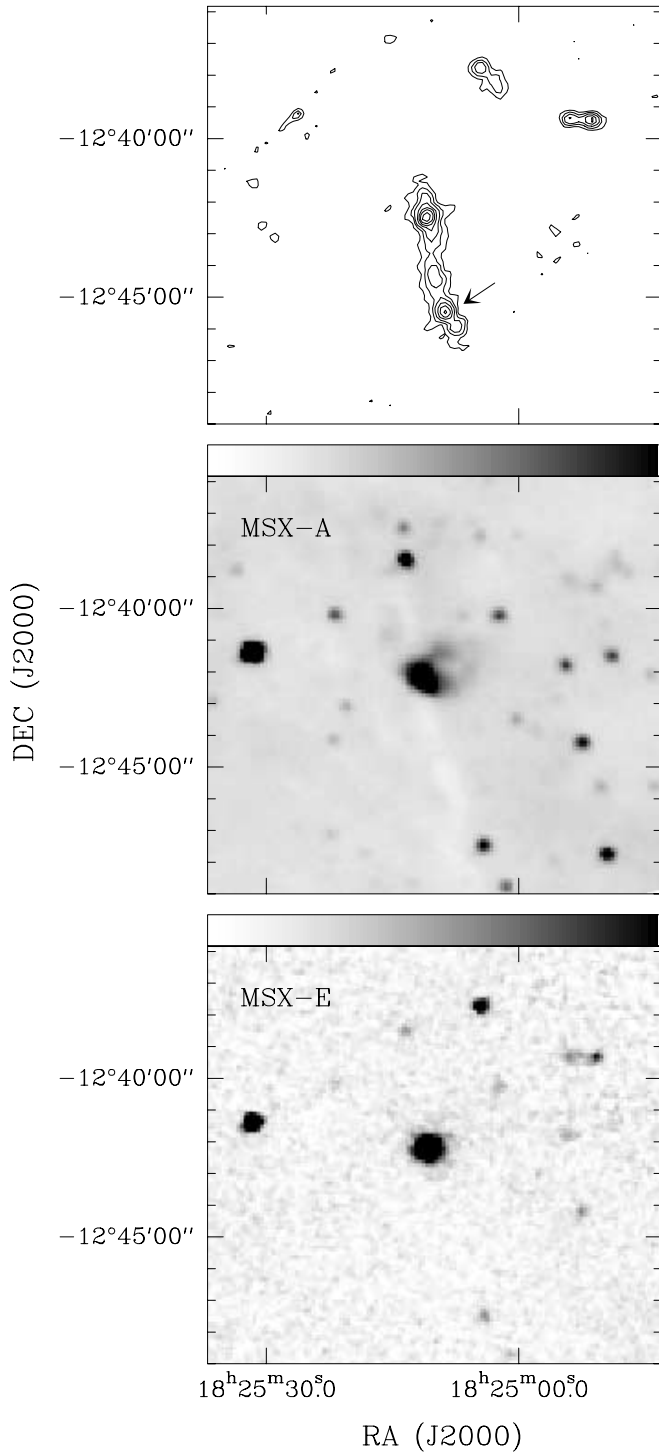


FIG. 3.—*Top*: Map of the 1.2 mm emission from a  $12' \times 15'$  region centered on IRAS 18223–1243. The arrow indicates the G18.606–0.076 massive and dense cold core. Contour levels are 0.1, 0.2, 0.3, 0.45, 0.60, 0.75, and  $0.95 \text{ mJy beam}^{-1}$ . *Middle*: Image of the *MSX* emission in the A broad band (6.8–10.8  $\mu\text{m}$ ). *Bottom*: Image of the *MSX* emission in the E broad band (18.2–25.1  $\mu\text{m}$ ).

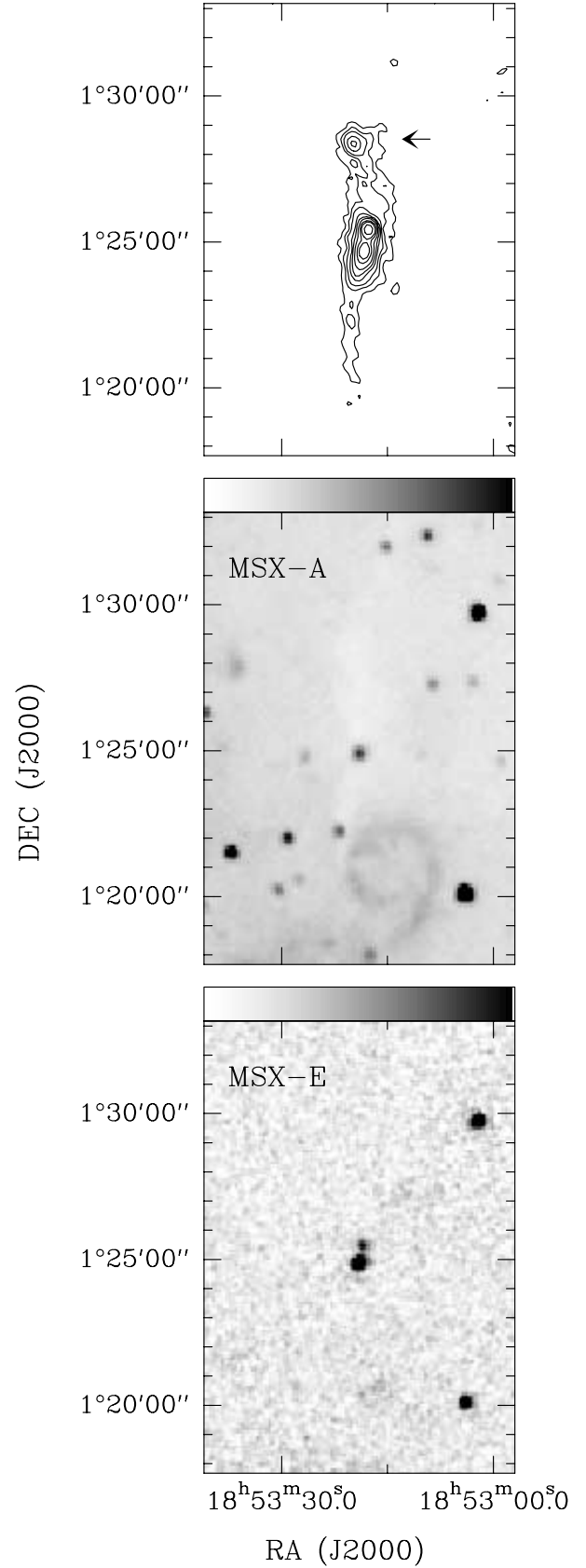


FIG. 4.—*Top*: Map of the 1.2 mm emission from a  $10' \times 15'$  region centered on IRAS 18507+0121. The arrow indicates the G34.458+0.121 massive and dense cold core. Contour levels are 1, 2, 3, 5, 7, 10, 15, 20, and  $30 \times 0.12 \text{ mJy beam}^{-1}$ . *Middle*: Image of the *MSX* emission in the A broad band (6.8–10.8  $\mu\text{m}$ ). *Bottom*: Image of the *MSX* emission in the E broad band (18.2–25.1  $\mu\text{m}$ ).

TABLE 1  
OBSERVED PARAMETERS OF 1.2 mm SOURCES

| SIMBA SOURCE<br>(1)  | PEAK POSITION      |                    | 1.2 mm       |                          | CS (2 → 1)                   |                                     |   |
|----------------------|--------------------|--------------------|--------------|--------------------------|------------------------------|-------------------------------------|---|
|                      | $\alpha$ (J2000.0) | $\delta$ (J2000.0) | Flux<br>(Jy) | $\theta_s^a$<br>(arcsec) | $V$<br>(km s <sup>-1</sup> ) | $\Delta v$<br>(km s <sup>-1</sup> ) | $\int T_{mb} dv$<br>(K km s <sup>-1</sup> ) |
|                      | (2)                | (3)                | (4)          | (5)                      | (6)                          | (7)                                 | (8)   |
| G305.136+0.068 ..... | 13 10 41.7         | -62 43 15.5        | 4.24         | 33                       | -36.4 ± 0.02                 | 4.15 ± 0.04                         | 4.62 ± 0.04                                 |
| G333.125-0.562.....  | 16 21 34.9         | -50 41 10.2        | 8.88         | 40                       | -58.5 ± 0.01                 | 3.90 ± 0.03                         | 3.32 ± 0.03                                 |
| G18.606-0.076.....   | 18 25 08.7         | -12 45 26.9        | 1.17         | 23                       | ...                          | ...                                 | ...   |
| G34.458+0.121 .....  | 18 53 19.8         | +01 28 21.8        | 2.55         | 26                       | 58.6 ± 0.01                  | 3.38 ± 0.03                         | 3.30 ± 0.03                                 |

NOTE.—Units of right ascension are hours, minutes, and seconds, and units of declination are degrees, arcminutes, and arcseconds.

<sup>a</sup> FWHM angular size.

observing time. We observed four blocks per source, achieving an rms noise level of typically 35 mJy beam<sup>-1</sup>. The data were reduced according to a standard procedure using the software package MOPSI, which included baseline subtraction and rejection of correlated sky noise. Flux calibration was performed using a sky-opacity correction and a counts-to-flux conversion factor derived from maps of Uranus. Uncertainties in the absolute calibration and pointing accuracy are estimated at 20% and 3'', respectively.

The molecular line observations were carried out at the SEST in 2003 March. We used the high-resolution acousto-optical spectrometers, which provided a channel separation of 43 kHz and a total bandwidth of 43 MHz. We mapped the CS (2 → 1) emission across regions of 2' in diameter, with angular spacings of 30'', centered at the peak of the dust cores. On-source integration time per map position was 3 minutes. We also observed at the peak position of the starless massive dense cores the emission in the CS (3 → 2) and CS (5 → 4) lines. System temperatures were typically ~200 K at 3 mm, ~290 K at 2 mm and ~430 K at 1 mm.

### 3. RESULTS

Using as a primary reference the 1.2 mm continuum emission maps from the survey of Faúndez et al. (2004), we made maps of the emission at mid-IR and far-IR wavelengths from the same regions using as databases the *MSX* (Price 1995) survey of the Galactic plane (Egan et al. 1998) at 8, 12, 15, and 22  $\mu$ m, and the *IRAS* all-sky survey at 12, 25, 60, and 100  $\mu$ m. A comparison between these maps yielded five massive ( $M > 400 M_{\odot}$ ) 1.2 mm dust cores, without emission (above the local background) in any of the *MSX* and *IRAS* bands. One of these objects corresponds to the NGC 6334 I(N) core (Gezari 1982), which has been extensively studied at millimeter and submil-

limeter wavelengths by Sandell (2000). Hereafter, we only concentrate on the four newly discovered massive cold cores.

Figures 1–4 (*top panel*) present maps of the 1.2 mm emission from regions of  $\sim 10'$ – $15'$  in size centered on the *IRAS* sources. Also shown in these figures are gray scale images of mid-IR emission in the A band (8  $\mu$ m; *middle panel*) and E band (22  $\mu$ m; *bottom panel*) of the *MSX* survey. The extended emission seen in the A band, which is sensitive to emission from polycyclic aromatic hydrocarbon (PAH) molecules (at 7.7 and 8.3  $\mu$ m), is likely to arise from photodissociated regions. An inspection of Figures 1–4 reveals the presence of 1.2 mm sources without counterparts in the *MSX* database. These 1.2 mm sources (marked by arrows in the top panels) are also undetected at far-IR wavelengths by the *IRAS*. Their positions, flux densities, and sizes are listed in Table 1.

The parameters derived from the 1.2 mm observations are summarized in Table 2. The cores are assumed to be at the same distance as the nearby *IRAS* sources (given in col. [2]). These correspond to kinematical distances derived by Faúndez et al. (2004), assuming a flat rotation curve and the standard IAU constants for the solar velocity and solar radius. They resolved the twofold ambiguity in kinematic distance for all four *IRAS* sources and concluded that they are located at the near distance. Errors in the distance to the cold cores, arising from either the small differences in velocities with respect to the *IRAS* cores or from the use of different rotation curves, are estimated to be of the order of  $\sim 20\%$ . Not enough data are available to make a precise determination of the dust temperature of the cores, although the lack of 100  $\mu$ m emission indicates that their temperatures are low ( $\leq 15$  K; Clark et al. 1991). Using the upper limits of the flux densities at *IRAS* wavelengths, constraining the sizes to those measured at 1.2 mm, and adopting a power-law index of 2 for the dust-opacity dependence with frequency,

TABLE 2  
DERIVED PARAMETERS

| SIMBA SOURCE<br>(1)  | 1.2 mm |      |       |                   |                     | CS (2 → 1) |                   |                     |
|----------------------|--------|------|-------|-------------------|---------------------|------------|-------------------|---------------------|
|                      | $D$    | $R$  | $T_d$ | $M^a$             | $n^a$               | $R$        | $M_{vir}$         | $n$                 |
|                      | (kpc)  | (pc) | (K)   | ( $M_{\odot}$ )   | (cm <sup>-3</sup> ) | (pc)       | ( $M_{\odot}$ )   | (cm <sup>-3</sup> ) |
| (2)                  | (3)    | (4)  | (5)   | (6)               | (7)                 | (8)        | (9)               |                     |
| G305.136+0.068 ..... | 3.4    | 0.27 | <16   | $1.1 \times 10^3$ | $2 \times 10^5$     | 0.30       | $1.1 \times 10^3$ | $2 \times 10^5$     |
| G333.125-0.562.....  | 3.5    | 0.34 | <17   | $2.3 \times 10^3$ | $2 \times 10^5$     | 0.68       | $2.2 \times 10^3$ | $3 \times 10^4$     |
| G18.606-0.076.....   | 3.7    | 0.20 | <15   | $4.0 \times 10^2$ | $2 \times 10^5$     | ...        | ...               | ...                 |
| G34.458+0.121 .....  | 3.8    | 0.24 | <17   | $7.8 \times 10^2$ | $2 \times 10^5$     | 0.64       | $1.5 \times 10^3$ | $2 \times 10^4$     |

<sup>a</sup> Lower limit.

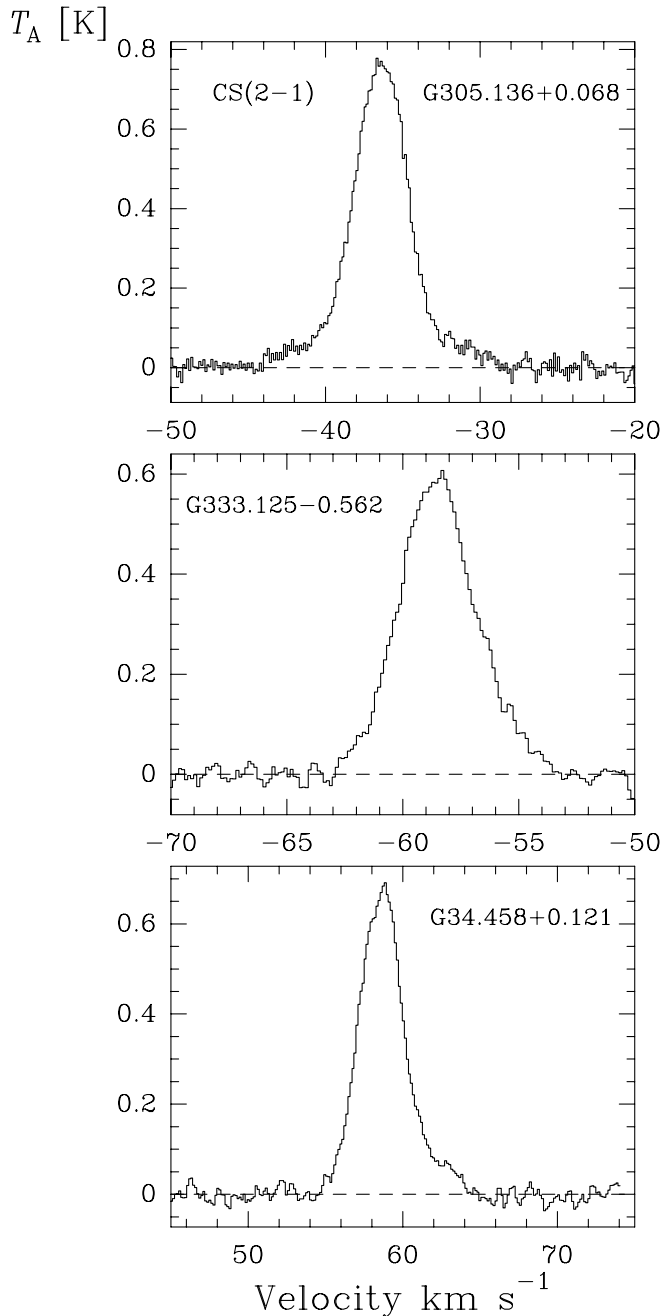


FIG. 5.—Spectra of the spatially integrated CS ( $2 \rightarrow 1$ ) line emission from the three observed cold massive dense cores.

a fit to the spectral energy distribution gives an upper limit on the dust temperature of typically 17 K. The masses of the cores, given in Table 2, column (5), were computed following Chini et al. (1987), adopting a dust opacity at 1.2 mm of  $1 \text{ cm}^2 \text{ g}^{-1}$  (Ossenkopf & Henning 1994), a dust-to-gas mass ratio of 0.01, and assuming that the cores have dust temperatures equal to the upper limit derived for the fit. The derived masses are in the range  $4 \times 10^2 - 2 \times 10^3 M_\odot$ . The densities derived from these masses and the radius given in Table 2, column (3), assuming that the cores have uniform densities, are typically  $\sim 2 \times 10^5 \text{ cm}^{-3}$ .

Figure 5 presents the integrated spectra of the CS ( $2 \rightarrow 1$ ) line emission from the three observed cold 1.2 mm dust cores. The spectra exhibit nearly Gaussian line profiles. The line center velocity, line width, and velocity-integrated brightness

temperature, determined from Gaussian fits to the spectra, are given in columns (6)–(8) of Table 1, respectively. The line widths are broad, typically  $\sim 4 \text{ km s}^{-1}$ , much larger than the thermal widths, indicating that these cores are highly turbulent and implying that their mean pressures are very high, typically  $\sim 3 \times 10^8 \text{ K cm}^{-3}$ . The large amount of support provided by the turbulent pressure allows the existence of cores in hydrostatic equilibrium with much larger densities than in low-mass cores. We note that the spectra of G305.136+0.068 show clear wing emission, which may indicate the presence of out-flowing gas.

The molecular line observations confirm that the 1.2 mm objects are associated with massive and dense molecular cores. The derived parameters from these observations are summarized in columns (7)–(9) of Table 2. The radius of the molecular cores, determined from maps of the CS ( $2 \rightarrow 1$ ) line emission, range from 0.3 to 0.6 pc. Assuming that the molecular cores are in virial equilibrium (MacLaren et al. 1988), we derive from the observed size and average line width in the CS ( $2 \rightarrow 1$ ) transition virial masses in the range  $1.1 \times 10^3$  to  $2.2 \times 10^3 M_\odot$ . The densities given in Table 2, column (9), were derived from the virial masses and the CS radius, assuming that the cores have uniform densities. Since the density in the cores is unlikely to be uniform, these values should be taken as rough estimates only. In fact, preliminary modeling of the CS emission using Monte Carlo analysis suggest that the massive and dense cold cores have density profiles with power-law indices of about  $-1$ . The physical parameters of the massive cores independently derived from the dust continuum and molecular line observations are in good agreement, indicating that freeze-out of molecules into grains is not important on these large scales.

#### 4. DISCUSSION

Our 1.2 mm survey toward massive star-forming regions have revealed the presence of massive ( $M > 400 M_\odot$ ) dust cores that are not seen in emission at either mid-IR or far-IR wavelengths. These dust cores have radii of 0.2–0.3 pc, masses in the range  $4 \times 10^2 - 2 \times 10^3 M_\odot$ , and densities of  $\sim 2 \times 10^5 \text{ cm}^{-3}$ . These physical properties are similar to those of the massive dense cores associated with *IRAS* sources reported by Faúndez et al. (2004). The temperatures of the 1.2 mm dust cores without emission at far-IR wavelengths are, however, significantly lower than that of the cores with embedded massive stars, which have temperatures of typically 32 K (Faúndez et al. 2004). It appears that a significant fraction of the total mass of the massive dense cold cores is in the form of molecular gas, as suggested by the similar values of the mass derived from the dust continuum emission (gas mass) and the virial mass (total mass) determined from the molecular line observations, indicating that the gas dominates the gravitational potential. Although we cannot conclude that the massive dense cold cores are starless, the lack of mid- to far-IR emission implies that they do not contain high-mass stars. Upper limits to the luminosity of these cores are typically  $2 \times 10^3 L_\odot$ . We hypothesize that the massive and dense cold cores reported here are likely to be in a stage before an internal luminosity source develops and will eventually collapse to form high-mass stars. To date there are only a few massive and dense starless cores already identified (Wyrowski et al. 1999; Sandell 2000).

Two of the 1.2 mm cold dust cores (G18.606–0.076 and G34.458+0.121) are part of long narrow filamentary structures. The filament associated with G18.606–0.076 has a

length of  $\sim 5'$ , a FWZP of  $\sim 45''$ , and breaks up into three, possibly four, condensations, one of which is associated with IRAS 18223–1243. The filament is clearly seen in the *MSX* A band image as a sink in the Galactic background emission, implying that it has an opacity at  $8\ \mu\text{m}$  greater than 1. Assuming a dust temperature of 15 K, we find that the filament extending south of IRAS 18223–1243 has a mass of  $1.4 \times 10^3 M_\odot$  and an average density of  $3 \times 10^4\ \text{cm}^{-3}$ .

The G34.458+0.121 dust core is located at the northern end of a filamentary structure that extends by  $\sim 9'$  in the north-south direction. The central region of this filament is associated with the massive star-forming region IRAS 18507+0121 (also known as G34.4+0.23). Maps of ammonia emission toward this region, made from observations with low angular resolution ( $90''$ ), show the presence of an ammonia cloud of  $\sim 2' \times 1'$ , elongated in the north-south direction (Miralles et al. 1994). The total molecular mass, determined assuming a distance of 3.9 kpc and an  $[\text{NH}_3/\text{H}_2]$  abundance ratio of  $10^{-6}$ , is  $\sim 10^3 M_\odot$ . Our observations at 1.2 mm show a double-peaked structure, with peaks separated by  $\sim 45''$ . The north component, located at  $\alpha = 18^{\text{h}}53^{\text{m}}17^{\text{s}}.71$ ,  $\delta = +01^{\circ}25'25''.1$  (J2000.0), has a flux density of 3.4 Jy, is unresolved by our observations, and is coincident with the 3 mm source G34.4+0.23 MM discovered by Shepherd et al. (2004). The south component is elongated in the north-south direction (FWHM sizes of  $87'' \times 31''$ , P.A.  $171^\circ$ ) and has a flux density of 16.9 Jy. Its peak position ( $\alpha = 18^{\text{h}}53^{\text{m}}18^{\text{s}}.31$ ,  $\delta = +01^{\circ}24'41''.4$  [J2000.0]) is coincident with the position of the UC H II region associated with IRAS 18507+0121 (Miralles et al. 1994). The interferometric observations of Shepherd et al. (2004) fully resolve out the dust emission from this extended component.

The masses of the G34.4+0.23 north and south cores, determined from the 1.2 mm observations and assuming a dust temperature of 28 K (Faúndez et al. 2004), are  $\sim 5.5 \times 10^2$  and  $\sim 2.7 \times 10^3 M_\odot$ , respectively. The *MSX* images (see Fig. 4) show the presence of energy sources within each of these two cores. Near-IR observations show that the G34.4+0.23 south core contains a cluster of young stars, whereas the G34.4+0.23 north core does not (Shepherd et al. 2004). These authors propose that the G34.4+0.23 north core harbors a deeply embedded massive protostar and suggest that the process of star formation in this core has taken place more recently than within the G34.4+0.23 south core. The newly discovered massive dense cold core reported here, located  $\sim 3.3$  north of G34.4+0.23, seems to be in a quiescent state, since it is not associated with any sign of star formation, and thus appears to be the youngest of the three cores within the filament. The G34.458+0.121 massive core may thus represent the analog to low-mass “class –1” cores.

What is the origin of massive dense cold cores? Are they formed by a gradual condensation process or produced by fast processes, e.g., by shocks within a turbulent medium? Important observational facts that have to be considered in addressing this question are the morphologies of the cores and

of their surroundings, both of which are likely to be useful indicators of the formation mechanism. Our observations, as well as those of Faúndez et al. (2004), suggest that filamentary structures play an important role in the process of formation of massive stars. The mechanisms by which filaments form are, however, not well understood. Numerical simulations (e.g., Klessen & Burkert 2000; Ostriker et al. 2001) show that filamentary structures occur as the result of fragmentation of a molecular cloud through turbulent motions. Filamentary structures can also be formed by fragmentation of magnetized sheetlike structures (Nakajima & Hanawa 1996). Whatever the mechanism of formation might be, once formed the filamentary structures are expected to fragment along their axis by gravitational instability, producing clumps and cores (Larson 1985; Fiege & Pudritz 2000; Tilley & Pudritz 2003). According to Fiege & Pudritz (2000), the critical wavelength for the separation of fragments is

$$\lambda_{\text{frag}} = 2.8 \left( \frac{\sigma_c}{0.5\ \text{km s}^{-1}} \right) \left( \frac{n_c}{10^4\ \text{cm}^{-3}} \right)^{-1/2} \left( \frac{k_{\text{max}}}{0.2} \right)^{-1} \text{ pc},$$

where  $n_c$  and  $\sigma_c$  are, respectively, the number density and the velocity dispersion at the center of the filament, and  $k_{\text{max}}$  is a dimensionless wavenumber ( $\leq 0.462$ ). We find that the average separation of the condensations within the filaments associated with G18.606–0.076 and G34.458+0.121 is 1.8 pc, in good agreement with the theoretical predictions for a filament density of  $3 \times 10^4\ \text{cm}^{-3}$ .

Two of the four 1.2 mm cold dust cores reported here (G305.136+0.068 and G333.125–0.562) appear as distinct isolated objects. The G305.136+0.068 core appears to be surrounded by an envelope of emission at  $8\ \mu\text{m}$ , indicating heating of its outer regions. The emission in the *MSX* A band is likely to arise from small grains and/or PAHs, both of which are excited by the Galactic UV radiation field. One possible explanation for the presence of isolated massive dust cores (see also Garay et al. 2003) is that dense cores are formed by a gradual dissipation of turbulent motions in larger clouds (Larson 1982). This process will cause the gravitational contraction of the large cloud while it still nearly remains near virial equilibrium, reducing its size and increasing its internal velocity dispersion. The gas is funneled down to the center of the core, where it is accreted by the central object at high rates. This hypothesis finds observational support in the fact that most UC H II regions—signposts of recently formed massive stars—are found at the center of massive dense cores (Garay et al. 2004).

L. B., G. G., and D. M. gratefully acknowledge support from the Chilean Centro de Astrofísica FONDAF 15010003. G. G. also acknowledges support from FONDECYT project 1010531.

#### REFERENCES

- Beuther, H., Schilke, P., Menten, K. M., Motte, F., Sridharan, T. K., & Wyrowski, F. 2002, *ApJ*, 566, 945  
 Bronfman, L., Nyman, L. Å., & May, J. 1996, *A&AS*, 115, 81  
 Chini, R., Krügel, E., & Wargau, W. 1987, *A&A*, 181, 378  
 Clark, F. O., Laureijs, R. J., & Prusti, T. 1991, *ApJ*, 371, 602  
 Egan, M. P., Shipman, R. F., Price, S. D., Carey, S. J., Clark, F. O., & Cohen, M. 1998, *ApJ*, 494, L199  
 Evans, N. J., II. 1999, *ARA&A*, 37, 311  
 Evans, N. J., II, Shirley, Y. L., Mueller, K. E., & Knez, C. 2002, in *ASP Conf. Ser. 267, The Earliest Stages of Massive Star Birth*, ed. P.A. Crowther (San Francisco: ASP), 17  
 Faúndez, S., Bronfman, L., Garay, G., Chini, R., May, J., & Nyman, L. A. 2004, *A&A*, in press  
 Fiege, J. D., & Pudritz, R. E. 2000, *MNRAS*, 311, 105  
 Garay, G., Brooks, K. J., Mardones, D., & Norris, R. P. 2003, *ApJ*, 587, 739  
 ———. 2004, *ApJ*, submitted

- Gezari, D. Y. 1982, *ApJ*, 259, L29  
Juvela, M. 1996, *A&AS*, 118, 191  
Klessen, R. S., & Burkert, A. 2000, *ApJS*, 128, 287  
Larson, R. B. 1982, *MNRAS*, 200, 159  
———. 1985, *MNRAS*, 214, 379  
MacLaren, I., Richardson, K. M., & Wolfendale, A. W. 1988, *ApJ*, 333, 821  
Miralles, M. P., Rodríguez, L. F., & Scalise, E. 1994, *ApJS*, 92, 173  
Mueller, K. E., Shirley, Y. L., Evans, N. J., II, & Jacobson, H. R. 2002, *ApJS*, 143, 469  
Nakajima, Y., & Hanawa, T. 1996, *ApJ*, 467, 321  
Ossenkopf, V., & Henning, Th. 1994, *A&A*, 291, 943  
Ostriker, E. C., Stone, J. M., & Gammie, C. F. 2001, *ApJ*, 546, 980  
Plume, R., Jaffe, D. T., & Evans, N. J., II. 1992, *ApJS*, 78, 505  
Plume, R., Jaffe, D. T., Evans, N. J., II, Martín-Pintado, J., & Gómez-Gonzalez, J. 1997, *ApJ*, 476, 730  
Price, S. D. 1995, *Space Sci. Rev.*, 74, 81  
Sandell, G. 2000, *A&A*, 358, 242  
Shepherd, D. S., Nurnberger, D. E. A., & Bronfman, L. 2004, *ApJ*, 602, 850  
Tilley, D. A., & Pudritz, R. E. 2003, *ApJ*, 593, 426  
Wyrowski, F., Schilke, P., Walmsley, C. M., & Menten, K. M. 1999, *ApJ*, 514, L43